Stem Cell Reports
Report
ISSCR
OPEN ACCESS

Lineage Tracing of Mammary Epithelial Cells Using Cell-Type-Specific Cre-Expressing Adenoviruses

Luwei Tao,[1,2] Maaike P.A. van Bragt,[1,2] Elizabeth Laudadio,[1,3] and Zhe Li[1,2,*]
[1]Division of Genetics, Brigham and Women's Hospital, Boston, MA 02115, USA
[2]Department of Medicine, Harvard Medical School, Boston, MA 02115, USA
[3]Harvard Stem Cell Institute, Cambridge, MA 02138, USA
*Correspondence: zli4@rics.bwh.harvard.edu
http://dx.doi.org/10.1016/j.stemcr.2014.04.004

SUMMARY

Lineage tracing using Cre/lox transgenic mice provides a powerful tool for studying normal mammary epithelial cell (MEC) development and the cellular origins of mammary tumors under physiological settings. However, generation of new transgenic mice for lineage-tracing purposes is often time consuming. Here, we report a lineage-tracing tool for MECs based on intraductal injection of lineage-specific Cre-expressing adenovirus (*Ad-Cre*). Using well-characterized promoters for *Keratin 8* and *Keratin 14*, we generated lineage-specific *Ad-Cre* lines for luminal and basal MECs, respectively. By pulse-chase lineage tracing using these *Ad-Cre* lines, we showed that luminal and basal lineages are largely self-sustained and that IRS1 and IRS2 are essential for maintaining the basal lineage; we also showed that heterogeneous mammary tumors can be induced from luminal MECs in mice carrying the *Etv6-NTRK3* fusion gene. Overall, we validated the *Ad-Cre* system as a promising and efficient tool for fate mapping of normal and malignant cells in adult tissues.

INTRODUCTION

Lineage tracing is a powerful tool for studying tissue development, homeostasis, and disease, and has provided unprecedented insights into stem cell biology (Kretzschmar and Watt, 2012). Previous lineage-tracing studies mostly relied on inducible Cre-estrogen receptor fusion protein (CreER)-expressing transgenic mice upon induction by tamoxifen. This inducible system was recently used for fate-mapping studies of mammary epithelial cells (MECs) under the physiological setting (Lafkas et al., 2013; Rios et al., 2014; Šale et al., 2013; van Amerongen et al., 2012; Van Keymeulen et al., 2011). However, wider application of this approach is limited by several factors. First, the choice of specific inducible CreER-expressing lines is often limited, and generating new mouse lines for this purpose can be time consuming. Second, most *CreER* mice do not target MECs exclusively, and for breast cancer modeling studies, their activities outside of the mammary gland (MG) may lead to systematic deficiency or unwanted tumor induction in other tissues, which could limit their use for studying MECs. Third, administration of tamoxifen may interfere with development of hormone-dependent tumors (e.g., mammary tumors), as well as normal MG development (Rios et al., 2014). Lastly, recent studies showed that the tamoxifen doses commonly used to induce Cre/lox recombination in mice might continue to label significant numbers of cells for weeks after tamoxifen treatment (Reinert et al., 2012) and that tamoxifen could change the behavior of stem cells (Zhu et al., 2013), both of which could affect interpretation of results from lineage-tracing experiments.

Adenovirus is a DNA virus, and it does not integrate into the host genome. It can infect both dividing and nondividing cells, leading to transient high-level protein expression (Anderson et al., 2000). Intraductal injection of adenovirus was previously shown to be an efficient way to transduce genes in MECs (Russell et al., 2003). Cre-expressing adenovirus (*Ad-Cre*) under the control of the constitutive *CMV* promoter (*Ad-CMV-Cre*) has been successfully used to induce cancer development in multiple organs (e.g., lung, ovary, and bladder; [DuPage et al., 2009; Flesken-Nikitin et al., 2003; Puzio-Kuter et al., 2009]). Recently, Sutherland et al. (2011) used cell-type-specific promoters and *Ad-Cre* to initiate small cell lung cancer development from different subsets of lung cells. We hypothesized that, similarly to the inducible CreER system, transient expression of Cre from adenoviral vectors could offer a temporal and spatial genetic-marking system for pulse-chase lineage-tracing studies in adult cells. In this study, we tested this approach in the MG by generating MEC lineage-specific *Ad-Cre* lines, and demonstrated that they can be used for MEC fate-mapping, gene loss-of-function, and cancer-induction studies in the native environment. This approach should also be suitable for lineage-tracing studies in other systems in which introduction of *Ad-Cre* is feasible.

RESULTS AND DISCUSSION

Genetic Marking of MECs by Intraductal Injection of *Ad-Cre*

It was demonstrated previously that mammary epithelium could be effectively transduced in vivo by adenovirus via

intraductal injection (Russell et al., 2003). We performed this procedure successfully in MGs of both adult virgin (Figure 1A) and 3-week-old (Figure 1B) female mice. Since puberty in mice occurs at ~4–6 weeks of age, this approach should allow us to introduce genetic changes into MECs during both pubertal development and adulthood. In pilot experiments, we injected *Ad-CMV-Cre* into #4 MGs of a conditional Cre-reporter mouse line, *Rosa26-lsl-YFP* (*R26YFP*). Cre expression from adenovirus triggered the excision of a floxed *Stopper* cassette in the *R26YFP* knockin allele, leading to permanent genetic marking of the infected cells and their progeny by yellow fluorescent protein (YFP; Figures 1C and 1D). The labeling efficiency of MECs, as measured by the percentage of YFP^+ cells 3 days after injection, ranged from 0.65% ± 0.05% to 19.23% ± 4.85%, corresponding to titers of *Ad-CMV-Cre* from 10^7 to 10^9 pfu/ml (Figure 1E). All major MEC subpopulations, including mature luminal cells (MLs, $CD31^-CD45^-TER119^-(Lin^-)CD24^{hi}CD29^+CD61^-$), luminal progenitors (LPs, $Lin^-CD24^{hi}CD29^+CD61^+$), and basal cells ($Lin^-CD24^{med}CD29^{hi}$), could be effectively labeled (Figure 1F). Only very minimal YFP-marked cells were detected in the stromal gate, which suggests that little viral leakage occurred, thus enabling us to study cell-autonomous effects in MECs (Figure 1F). Since the needle used for injection might have come in contact with skin surrounding the nipple, we performed immunofluorescence (IF) staining of tissues in this area. We only detected YFP^+ cells in the mammary ducts directly adjacent to the skin, as well as a few YFP^+ stromal cells; no skin cells were found to be YFP^+ (Figure S1A available online). Using flow cytometry and PCR for genomic DNA, we did not detect Cre-mediated excision in the *R26YFP* allele in tissues outside of the MG (Figures S1B–S1D), further confirming the MEC specificity of this approach. Lastly, since it was reported that intratracheal administration of *Ad-Cre* to the mouse lung could lead to clearance of infected lung cells, possibly due to an immune response (Meuwissen et al., 2001), we checked mammary tissues at various time points after intraductal injection of *Ad-Cre*. We did not observe any significant inflammatory response (Figure S1E), consistent with a previous study (Russell et al., 2003).

To assess the transient expression nature of adenovirus in vivo, we measured the duration of adenovirus-mediated gene expression in MECs by intraductally injecting *CMV-GFP* adenovirus (*Ad-CMV-GFP*) into wild-type FVB females. We found that at day 2 postinjection, 14.77% ± 4.60% GFP^+ cells were detected in the injected MGs; this number quickly dropped to 3.70% ± 1.48% at 1 week after injection, and to zero at 2 weeks postinjection (Figure 1G). We reason that Cre expression from the same adenoviral system should follow a similar kinetics and thus serves a similar purpose as the inducible *CreER* mice.

MEC Lineage Tracing Using Cell-Type-Specific *Ad-Cre* Lines

To target different MEC subsets, we generated lineage-specific *Ad-Cre* lines by using the same adenoviral backbone as *Ad-CMV-Cre* coupled with a cell-type-specific promoter to drive nlsCre (nls: nuclear localization sequence) expression. For the luminal lineage, we used the mouse *Keratin 8* (*K8*) promoter (Van Keymeulen et al., 2011) and generated *Ad-K8-nlsCre* virus. Three days after *Ad-K8-nlsCre* injection into *R26YFP* females, we found that *Ad-K8-nlsCre* specifically led to YFP labeling of luminal MECs (Figure 2Ab), including both MLs and LPs (Figure 2Ad). By IF staining of sorted YFP^+ cells or MG sections from the injected *R26YFP* females, we confirmed that the YFP^+ cells were exclusively $K8^+K14^-$ luminal cells (Figures 2C and S2D). To test the long-term labeling efficiency, we chased *R26YFP* females injected with *Ad-K8-nlsCre* for 1.5 months. At this stage, we found that YFP^+ cells could still be detected robustly and all YFP^+ cells remained restricted to the luminal gate (Figure 2Af). A similar observation was made even when the injected mice were chased further to 6 months (Figure S2A). These data suggest that the $K8^+$ luminal lineage contains self-sustained, long-lived MECs. Next, *Ad-K8-nlsCre*-injected *R26YFP* females were bred to trigger alveolar differentiation. At midgestation, we found that *Ad-K8-nlsCre*-marked YFP^+ luminal cells contributed to luminal cells in both lobules and main collecting ducts (Figures 2D and S2B). A previous in vivo lineage-tracing study using *K8-CreERT2* mice showed that in adult MGs, the luminal and basal lineages were maintained by their own unipotent stem cells (Van Keymeulen et al., 2011). Although a more recent lineage-tracing study provided evidence for a contribution of bipotent basal stem cells to the luminal lineage in vivo, it also revealed long-lived LPs that could contribute to maintenance of the luminal lineage (Rios et al., 2014). The results from our *Ad-K8-nlsCre* approach agreed with these findings, showing that the luminal lineage, including both ductal and alveolar luminal cells, could be self-sustained by luminal lineage-restricted stem cells or long-lived progenitors.

To mark the basal lineage, we used the human *Keratin 14* (*K14*) promoter to direct nlsCre expression via adenovirus (*Ad-K14-nlsCre*) (Sugihara et al., 2001). By intraductally injecting *Ad-K14-nlsCre* into *R26YFP* females, we found that most YFP^+ cells were restricted to the basal gate; however, a small population of YFP^+ cells could also be detected in the luminal gate (Figure 2Bb). Upon a long-term chase (1.5 months), we found that *Ad-K14-nlsCre*-marked YFP^+ basal and luminal cells were both maintained (Figure 2Bf). To determine the identities of the YFP^+ cells, we sorted YFP^+ cells in the luminal or basal gate from *R26YFP* females 3 days after *Ad-K14-nlsCre* injection, and stained them for K8 and K14. We found that YFP^+ cells sorted from the basal

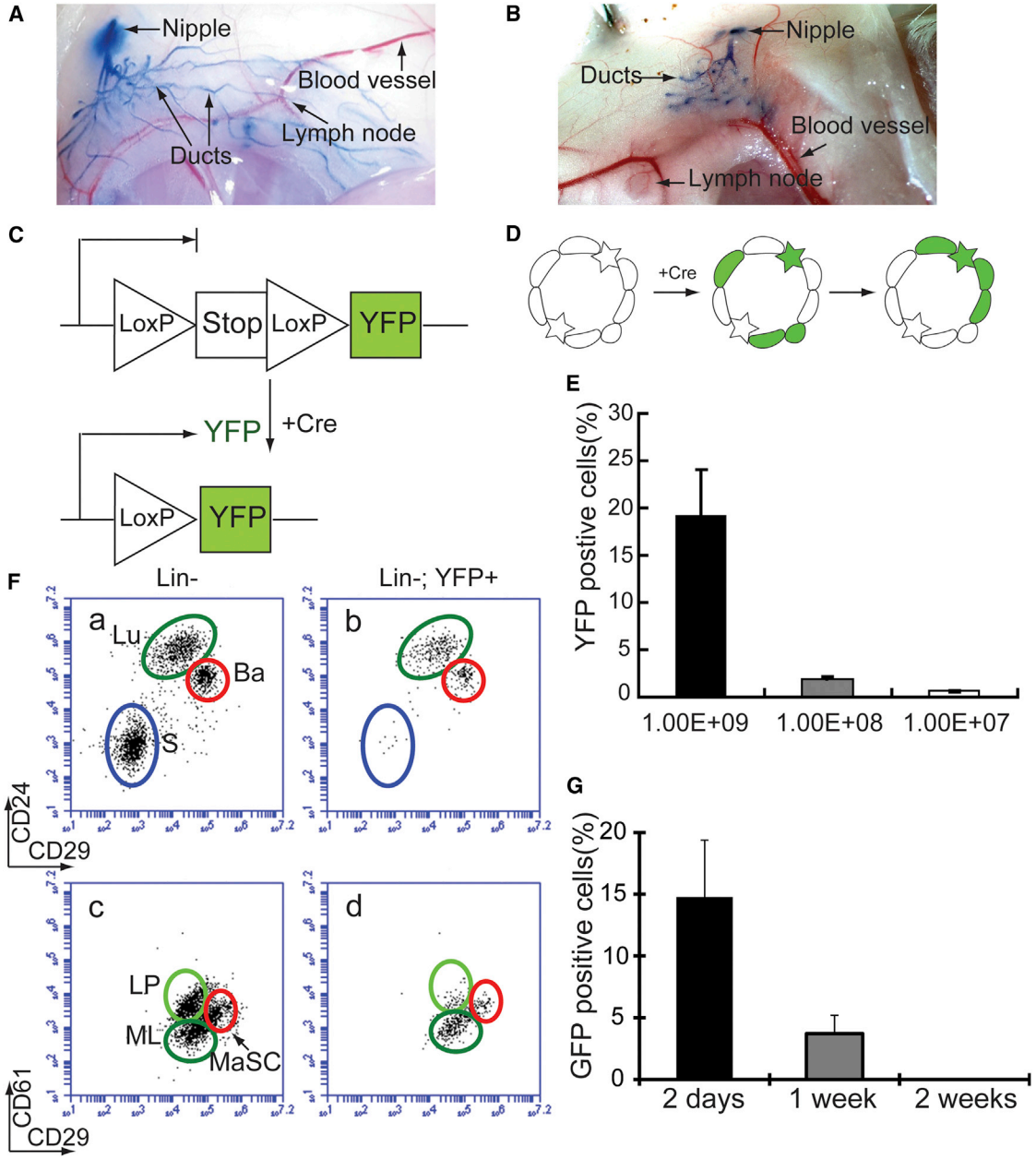

Figure 1. Genetic Marking of MECs by Intraductal Injection of *Ad-Cre*

(A and B) Intraductal injection of trypan blue dye into adult (A) and 3-week-old (B) female mice.

(C) Schematic diagram of *R26YFP* reporter activation upon Cre-mediated excision of a floxed *Stopper* (Stop) cassette.

(D) Schematic diagram of lineage-tracing strategy using intraductal injection of *Ad-Cre*. Green star designates a YFP-marked stem cell; other green cells refer to more differentiated MECs.

(E) Different efficiencies of Cre-mediated recombination (measured as % YFP^+ cells) achieved by using different titers of *Ad-CMV-Cre*.

(F) Flow-cytometric analysis of *R26YFP* females 3 days after *Ad-CMV-Cre* intraductal injection. Luminal cells (Lu), including luminal progenitors (LP) and mature luminal cells (ML), and basal/myoepithelial cells (Ba), including mammary stem cells (MaSCs), can be labeled by YFP upon *Ad-Cre* induction. Very few stromal cells (S) were labeled by this approach.

(G) Intraductal injection of *Ad-CMV-GFP* into FVB mice showing transient GFP expression in MGs. In (E) and (G), n = 3 (injected MGs). Data were reported as mean ± SEM.

See also Figure S1.

gate were exclusively $K8^-K14^+$ basal cells (Figure S2E). In contrast, the smaller subpopulation of YFP^+ cells sorted from the luminal gate were entirely $K8^+K14^-$, suggesting that a small portion of luminal cells were indeed labeled by *Ad-K14-nlsCre* (Figure S2F). Next, *R26YFP* females were marked by *Ad-K14-nlsCre* at the nulliparous stage and either remained virgins or went through pregnancy. By IF staining of their MG sections, we found that *Ad-K14-nlsCre*-marked basal cells contributed to both alveolar and ductal basal/myoepithelial cells (Figures 2E, 2F, and S2C). A small portion of YFP^+ MECs induced by *Ad-K14-nlsCre* also contributed to lobular and ductal luminal cells (Figure 2G). To determine the cellular origins of these labeled luminal cells, we performed a detailed clonal analysis (Figures 2H and S2G–S2J). We counted YFP^+ clones in the injected MGs at 3 days, 3 weeks, and 7 weeks after *Ad-K14-nlsCre* injection, and classified them into three categories: K14-only clones ($K14^+K8^-$), K8-only clones ($K8^+K14^-$), and mixed clones containing both cell types. We found that generally, $K14^+$ clones and $K8^+$ clones were labeled independently of each other (Figures 2H and S2G). Upon a 7-week chase, ~70% K14-only basal clones, 20% K8-only luminal clones, and 10% mixed clones were observed (Figure S2G). These data, combined with those obtained from *Ad-K8-nlsCre*-based lineage tracing, suggest that the $K14^+$ basal lineage is also self-sustained and may not contribute significantly to the luminal lineage in the short term. However, our data (e.g., showing the presence of mixed clones and a slight increase in the percentages of K8-only and mixed multicell clones upon a 7-week chase; Figure 2H) also do not exclude the possibility that rare $K14^+$ basal MECs can make a long-term contribution to the luminal lineage under the physiological setting, as demonstrated recently (Rios et al., 2014). Since the mixed clones we observed may also have resulted from the fusion of two independently labeled basal and luminal clones that were in a close proximity, three-dimensional analyses at much lower clonal densities will be required before we can precisely assess the cellular origin of these putative mixed clones.

IRS1 and IRS2 Are Essential for Maintaining the Basal Lineage

To determine whether lineage-specific *Ad-Cre* can be used to study the cell-autonomous function of genes or signaling pathways, we used *Ad-K8-nlsCre* and *Ad-K14-nlsCre* to study the role of insulin growth factor/insulin receptor substrate (IGF/IRS) signaling in adult MECs. During development, the IGF pathway is a primary mediator of the Growth Hormone pathway, which stimulates terminal end bud formation and ductal elongation (Kelly et al., 2002; Kleinberg and Ruan, 2008). Intracellular transduction of IGF and Insulin signaling are both mediated by two adaptor proteins, IRS1 and IRS2, through tyrosine phosphorylation (Dearth et al., 2007; Heckman et al., 2007). Abnormal activation of IGF signaling is closely associated with increased breast cancer risk (de Ostrovich et al., 2008).

Both IRS1 and IRS2 were previously shown to play important roles during embryonic MG development (Chan and Lee, 2008; Heckman et al., 2007). Postnatally, both *Irs1* and *Irs2* null MGs are normal, possibly because they compensate for each other (Chan and Lee, 2008; Heckman et al., 2007). We previously generated *Irs1/Irs2* double conditional knockout mice with the *R26YFP* reporter (*$Irs1^{L/L}$;$Irs2^{L/L}$;R26YFP*) and used *K14-Cre* and *MMTV-Cre* mouse lines to disrupt them in MECs (Figure S3A). Although the MGs of these mice looked largely normal by both histological (Figure S3B) and flow-cytometric (Figure S3C) analyses, by characterizing the Lin^-YFP^+ cells (i.e., *Irs1/2* null cells), we found that both models exhibited significantly reduced percentages of Lin^-YFP^+ *Irs1/2* null cells (Figures S3C and S3D), suggesting a growth defect of *Irs1/2* double-knockout MECs. In particular, in the *K14-Cre* model, which induced *Irs1/2*-loss in a lot more basal cells than the *MMTV-Cre* model, disruption of IGF/IRS signaling dramatically reduced the percentage of Lin^-YFP^+ basal cells (Figures S3C and S3E), suggesting that the basal lineage may be more dependent on this pathway for its survival and/or proliferation than luminal cells. However, since both *K14* and *MMTV* promoters are also active during embryonic development, one cannot differentiate the effects of *Irs1/2* loss on embryonic MEC development from those of adult MEC maintenance by using conventional *K14-Cre* or *MMTV-Cre* mice.

To determine whether IGF/IRS signaling is required for maintenance of each MEC lineage in adults, we injected *Ad-K8-nlsCre* or *Ad-K14-nlsCre* into adult *$Irs1^{L/L}$;$Irs2^{L/L}$;R26YFP* nulliparous females. Three days after injection, we found that the *$Irs1^{L/L}$;$Irs2^{L/L}$;R26YFP* mice showed similar YFP-labeling efficiencies compared with *R26YFP*-only control females (Figures 3A and 3B). However, 3 weeks after injection, whereas a similar level of YFP^+ cells (compared with the initial labeling) could be detected in *R26YFP* control females, in *$Irs1^{L/L}$;$Irs2^{L/L}$;R26YFP* females, the percentages of YFP^+ cells induced by either *Ad-K8-nlsCre* or *Ad-K14-nlsCre* injection decreased significantly (Figures 3A–3C). These data suggest that IGF/IRS signaling is also essential for maintaining the homeostasis of both the luminal and basal lineages in adult MGs. We also noted that *Ad-K14-nlsCre*-labeled YFP^+ basal cells almost completely disappeared after 3 weeks (Figure 3C, compare red circle in p with those in l and n), whereas a few *Ad-K14-nlsCre*-labeled or *Ad-K8-nlsCre*-labeled YFP^+ luminal cells were still present after a 3-week chase (Figure 3C, compare green circles in h or p with those in d and f, or in l and n, respectively). These data agree with our findings from the *K14-Cre* and *MMTV-Cre* conditional knockout mice, and suggest that basal cells are more

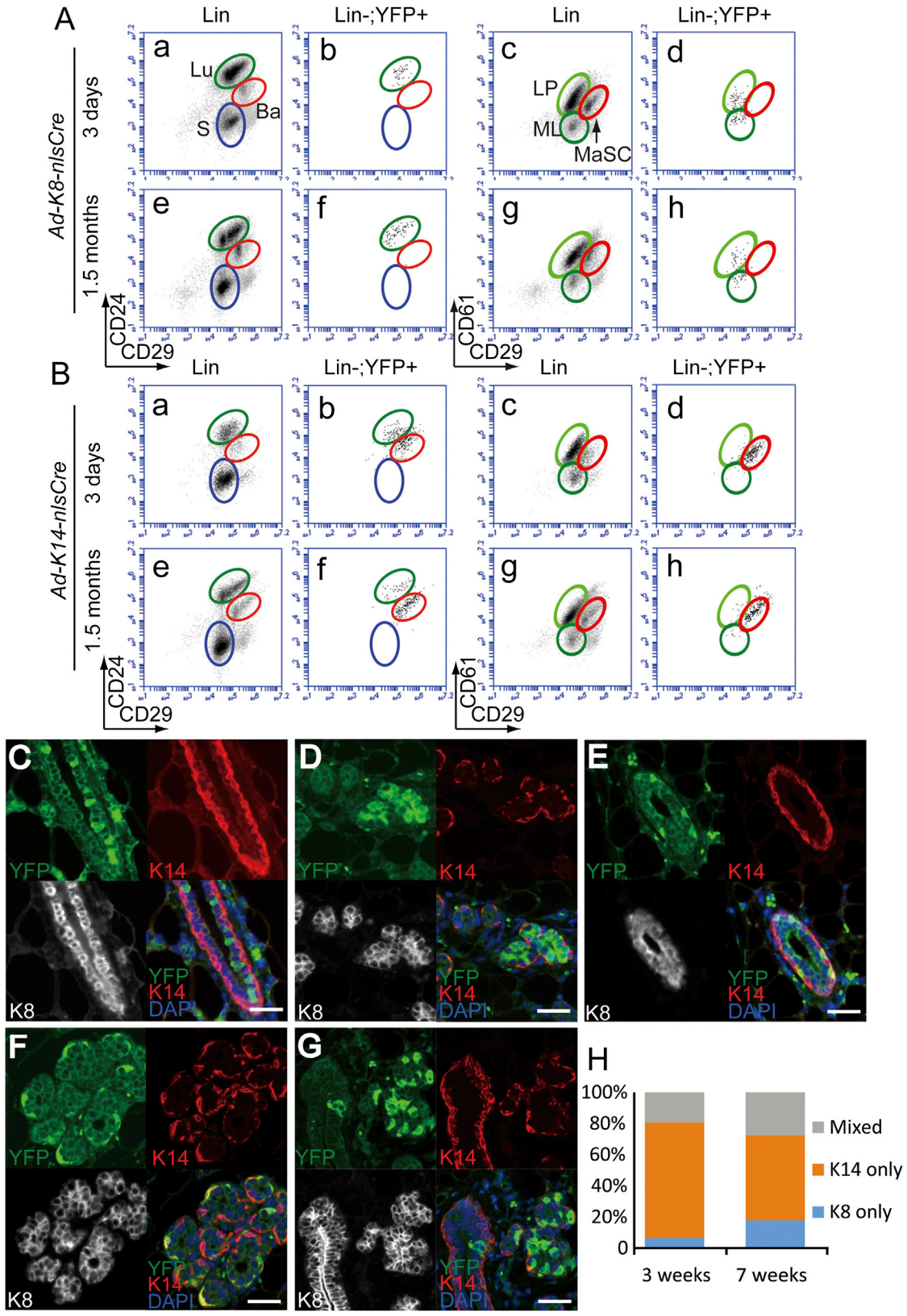

(legend on next page)

sensitive to loss of IGF/IRS signaling and that this pathway is essential for maintaining the basal lineage in vivo. Taken together, these results show that the lineage-specific *Ad-Cre* system enabled us to quickly study the functions and interactions of different genes and signaling pathways in a cell-autonomous manner.

Studying the Cellular Origin of Mammary Tumors by Using Lineage-Specific *Ad-Cre*

Since Sutherland et al. (2011) were able to initiate small cell lung cancer using *Ad-Cre*, we hypothesized that our cell-lineage-specific *Ad-Cre* viruses would allow us to study the cellular origin and transformation process of mammary tumorigenesis. To test this, we injected *Ad-K8-nlsCre* into the mammary ducts of mice carrying the *Etv6-NTRK3* (*EN*) conditional knockin allele we generated previously (Li et al., 2007). *EN* fusion oncogene, a product from t(12;15)(p13;q25) chromosome translocation, produces a chimeric tyrosine kinase that is characteristic of human secretory breast carcinoma (Tognon et al., 2002). Previously, commonly used MEC-specific Cre-expressing mouse lines, including *MMTV-Cre*, *K14-Cre*, and *Wap-Cre*, were applied to activate *EN* expression. However, due to activity outside of the MGs, *MMTV-Cre* or *K14-Cre*-driven *EN* activation led to animal lethality before any mammary tumor developed. Only *Wap-Cre* successfully induced activation of *EN* in alveolar progenitors in MGs, leading to the development of mammary tumors with 100% penetrance (Li et al., 2007).

We utilized *Ad-K8-nlsCre* for tumor induction in *EN*/+ females through intraductal injection. In all injected *EN*/+ mice, we did not detect any complication or malignancy in other tissues outside of the MG, including skin surrounding the injected nipple area. All injected *EN*/+ females developed multifocal mammary tumors in the injected glands with a tumor-free latency similar to that observed in *Wap-Cre;EN* females (Figure 4A). Cre-mediated activation of the *EN* knockin allele (i.e., removal of a floxed *Stopper* cassette) was confirmed by PCR using tumor genomic DNA (Figures 4B and S4A), suggesting that the development of mammary tumors was indeed driven by EN. IF staining of the induced tumors for K8 and K14 showed that two tumor types that developed in the previous *Wap-Cre;EN* model (Li et al., 2007) were recapitulated in the injected females, including type 1 tumors composed of $K8^+$ luminal tumor cells surrounded by $K14^+K5^+$ basal tumor cells ("bilineage," 7 out of 14 tumors), and a type 2 less differentiated tumor comprised of $K8^+K14^+K5^-$ cells ("double positive," 1 out of 14) (Figures 4C and S4B). Interestingly, in the injected females, a new type of tumor (type 3 "luminal," 6 out of 14; Figures 4C and S4B) consisting of predominantly $K8^+K14^-K5^-$ luminal tumor cells was also detected. All of these tumors were negative or weakly positive (e.g., type 1) for estrogen receptor (Figure S4B).

In virgin females, *Wap-Cre* (either from the transgenic mouse or via adenovirus) labeled a population of preexisting unipotent luminal stem or long-lived progenitor cells committed to the alveolar fate, and intraductal injection of *Wap-Cre* adenovirus into *EN*/+ females led to the development of type 1 and type 2 mammary tumors identical to those in *Wap-Cre;EN* females (M.P.A.v.B., L.T., and Z.L., unpublished data). As K8 is a pan-luminal marker, *Ad-K8-nlsCre* is expected to mark not only *Wap-Cre*-labeled alveolar luminal stem/progenitor cells but also other luminal cell types. Thus, our *Ad-Cre*-based tumor study suggests that EN oncoprotein is capable of transforming multiple luminal MEC subsets. Furthermore, due to the short latency of EN-induced mammary tumorigenesis (Figure 4A), our data are consistent with a model in which multiple subpopulations of luminal cells can serve as cells of origin, and distinct cellular origins contribute to the heterogeneity of breast cancer.

EXPERIMENTAL PROCEDURES

Adenovirus Shuttle Vector Construction and Adenovirus Production

Ad-CMV-Cre, *Ad-CMV-GFP*, promoterless adenoviral shuttle vector (pacAd5 K-NpA), and the packaging vector [pAd5(9.2-100)sub360]

Figure 2. MEC Lineage Tracing Using Cell-Type-Specific *Ad-Cre* Lines

(A) *Ad-K8-nlsCre* specifically labeled luminal epithelial cells (Lu), including mature luminal cells (ML) and luminal progenitors (LP), 3 days (a–d) and 1.5 months (e–h) after injection.

(B) *Ad-K14-nlsCre*-labeled cells were mostly basal/myoepithelial cells (Ba, including MaSC) 3 days (a–d) and 1.5 months (e–h) after injection. A small portion of luminal cells were also labeled by *Ad-K14-nlsCre*.

(C–G) IF staining of MGs after various chase durations for YFP^+ MECs upon pulse labeling by *Ad-Cre* injection at the nulliparous stage.

(C) Nulliparous MG 3 weeks after *Ad-K8-nlsCre* injection.

(D) Midgestation MG after *Ad-K8-nlsCre* injection. *Ad-K8-nlsCre*-induced YFP^+ cells contributed to alveolar formation.

(E) Nulliparous MG 3 weeks after *Ad-K14-nlsCre* injection.

(F and G) Midgestation MGs after *Ad-K14-nlsCre* injection. *Ad-K14-nlsCre*-induced YFP^+ cells contributed to alveolar myoepithelial cells (F) and both ductal and alveolar luminal cells (G). Scale bars, 50 μm.

(H) YFP-marked multicell clones (at least three cells per clone) induced by *Ad-K14-nlsCre* subdivided based on K8 and K14 expression patterns were quantified as K8-only clones, K14-only clones, or mixed clones.

See also Figure S2.

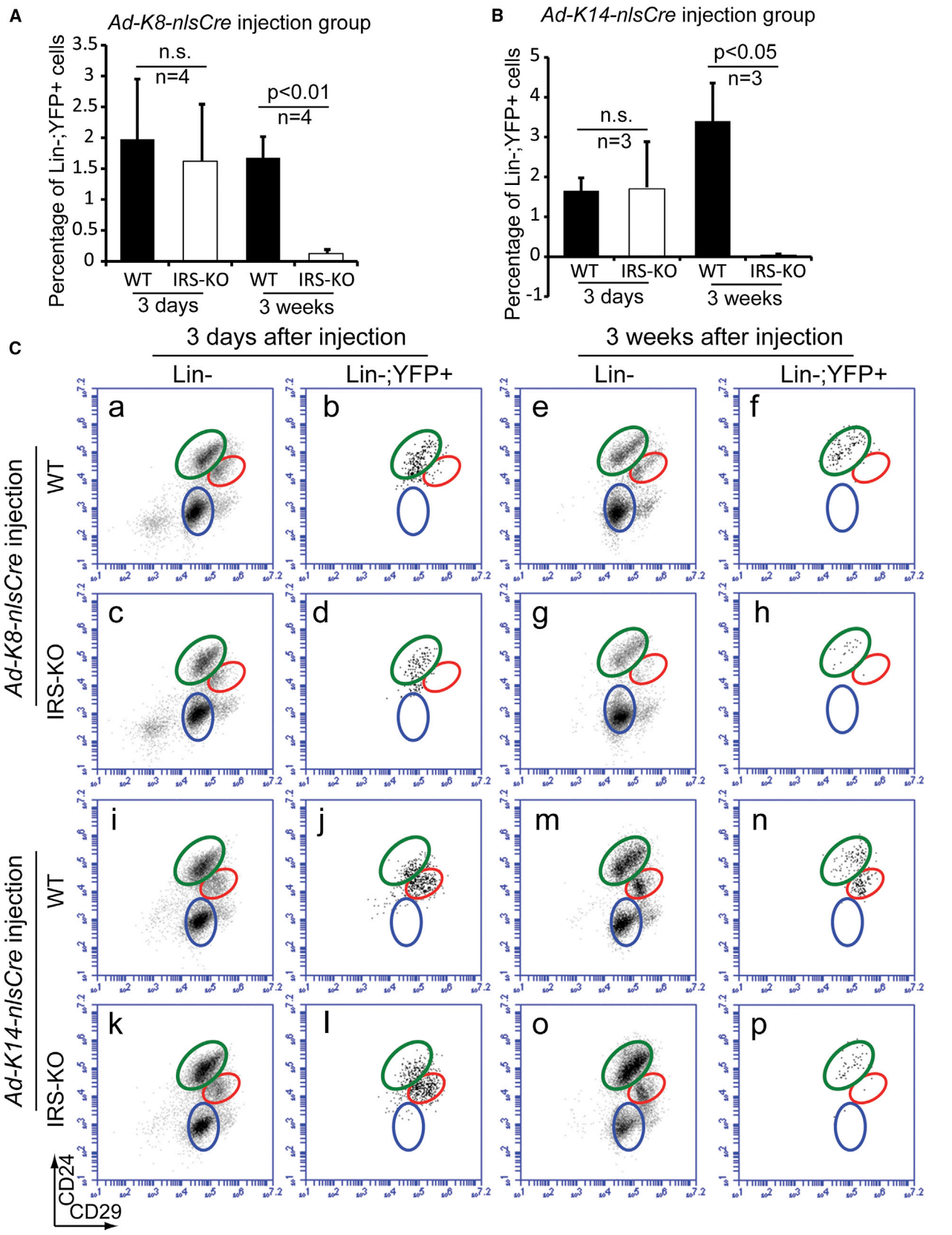

(legend on next page)

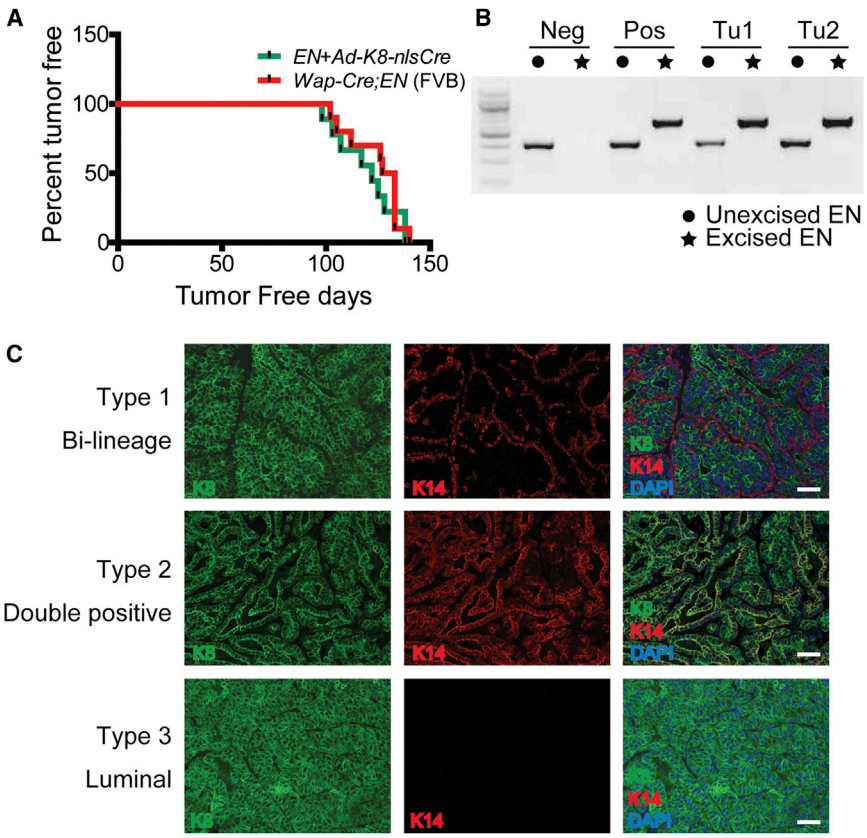

Figure 4. Tumor Induction Using the *Ad-Cre* Approach

(A) Kaplan-Meier curves showing mammary tumor development in *EN* knockin virgin female mice injected with *Ad-K8-nlsCre* (n = 9) and in *Wap-Cre;EN* virgin females (n = 10). All mice were under the pure FVB background.

(B) Cre-mediated activation of the *EN* conditional knockin allele in tumor cells was confirmed by PCR. The locations of the primers used to detect unexcised and excised *EN* alleles are indicated in Figure S4A.

(C) Three types of tumor derived from *EN/+* mice injected with *Ad-K8-nlsCre* as revealed by K8 and K14 IF staining. Scale bars, 50 μm.

See also Figure S4.

were obtained from the Gene Transfer Core of the University of Iowa (Anderson et al., 2000). nlsCre was amplified from pHR-CMV-nlsCRE plasmid (Addgene). Mouse *K8* promoter was amplified from mouse genomic DNA. Human *K14* promoter was amplified from K14-luciferase plasmid (Sugihara et al., 2001). Crude *Ad-K8-nlsCre* and *Ad-K14-nlsCre* were purified using the Adenopure purification kit (Puresyn).

Mice

R26YFP and *MMTV-Cre* mice were purchased from The Jackson Laboratory. *K14-Cre* and *Wap-Cre* mice were obtained from the MMHCC Repository. *Etv6-NTRK3* (*EN*) conditional knockin mice, as well as *Irs1* and *Irs2* conditional knockout mice, were described previously (Guo et al., 2009; Li et al., 2007). Adenoviruses were introduced into their mammary ducts via intraductal injection. All studies involving mice were approved by our institutional animal care and use committee, and performed in accordance with the relevant protocol.

MEC Preparation, Flow Cytometry, and Sorting

Single-cell suspensions of MECs were prepared as previously described (Shackleton et al., 2006). After antibody staining, flow-cytometric analysis was performed on Accuri 6 and DXP11 flow cytometers. Cell sorting was performed on a BD Aria.

Immunostaining and Clonal Analysis

Mammary tissues were fixed in 10% buffered formalin (Fisher), embedded in paraffin, and sectioned. IF and immunohistochemistry staining were performed on 6 μm paraffin sections for the indicated antibodies by standard procedures. Clonal analysis was performed on MG sagittal sections stained with YFP, K8, and K14 antibodies.

Figure 3. IRS1 and IRS2 Are Essential for Maintaining the Basal Lineage

(A and B) Bar graphs showing the percentages of YFP$^+$ cells. *Irs1$^{L/L}$;Irs2$^{L/L}$;R26YFP* (IRS-KO) and *R26YFP*-only (WT) control females were injected with *Ad-K8-nlsCre* (A) or *Ad-K14-nlsCre* (B), and YFP$^+$ cells were measured by flow cytometry 3 days or 3 weeks after injection. Data were reported as mean ± SEM. n.s., not significant.

(C) Flow-cytometric analysis of YFP$^+$ cells in *Irs1$^{L/L}$;Irs2$^{L/L}$;R26YFP* and *R26YFP*-only control females injected with *Ad-K8-nlsCre* (a–h) or *Ad-K14-nlsCre* (i–p). Both luminal cells (compare f and h) and basal/myoepithelial cells (compare n and p) decreased significantly 3 weeks after *Ad-Cre* injection. In particular, in *Ad-K14-nlsCre* injection group (compare n and p), the decrease in YFP$^+$ basal/myoepithelial cells was much more profound than that in YFP$^+$ luminal cells.

See also Figure S3.

Statistical Analysis

A Student's t test was used for statistical analysis. Data were reported as mean ± SEM.

SUPPLEMENTAL INFORMATION

Supplemental Information includes four figures and Supplemental Experimental Procedures and can be found with this article online at http://dx.doi.org/10.1016/j.stemcr.2014.04.004.

ACKNOWLEDGMENTS

We are grateful to Grigoriy Losyev and Yiling Qiu for expert technical assistance with FACS sorting, Dr. Beverly Davidson and the University of Iowa Gene Transfer Vector Core for pacAd5 K-NpA, Dr. Bogi Andersen for K14-luciferase plasmid, and Drs. Morris White and Xiaocheng Dong for *Irs1/2* conditional knockout mice. This research was supported by a K99/R00 grant from the NCI (CA126980), a Seed Grant and Cancer Program Pilot Grant from Harvard Stem Cell Institute, a Milton Fund Award from Harvard University, a Hearst Foundation Young Investigator Award from Brigham and Women's Hospital (BWH), startup funds from BWH, and NIH grant R01 HL107663 to Z.L.

Received: December 8, 2013
Revised: April 8, 2014
Accepted: April 9, 2014
Published: May 8, 2014

REFERENCES

Anderson, R.D., Haskell, R.E., Xia, H., Roessler, B.J., and Davidson, B.L. (2000). A simple method for the rapid generation of recombinant adenovirus vectors. Gene Ther. *7*, 1034–1038.

Chan, B.T., and Lee, A.V. (2008). Insulin receptor substrates (IRSs) and breast tumorigenesis. J. Mammary Gland Biol. Neoplasia *13*, 415–422.

de Ostrovich, K.K., Lambertz, I., Colby, J.K., Tian, J., Rundhaug, J.E., Johnston, D., Conti, C.J., DiGiovanni, J., and Fuchs-Young, R. (2008). Paracrine overexpression of insulin-like growth factor-1 enhances mammary tumorigenesis in vivo. Am. J. Pathol. *173*, 824–834.

Dearth, R.K., Cui, X., Kim, H.J., Hadsell, D.L., and Lee, A.V. (2007). Oncogenic transformation by the signaling adaptor proteins insulin receptor substrate (IRS)-1 and IRS-2. Cell Cycle *6*, 705–713.

DuPage, M., Dooley, A.L., and Jacks, T. (2009). Conditional mouse lung cancer models using adenoviral or lentiviral delivery of Cre recombinase. Nat. Protoc. *4*, 1064–1072.

Flesken-Nikitin, A., Choi, K.C., Eng, J.P., Shmidt, E.N., and Nikitin, A.Y. (2003). Induction of carcinogenesis by concurrent inactivation of p53 and Rb1 in the mouse ovarian surface epithelium. Cancer Res. *63*, 3459–3463.

Guo, S., Copps, K.D., Dong, X., Park, S., Cheng, Z., Pocai, A., Rossetti, L., Sajan, M., Farese, R.V., and White, M.F. (2009). The Irs1 branch of the insulin signaling cascade plays a dominant role in hepatic nutrient homeostasis. Mol. Cell. Biol. *29*, 5070–5083.

Heckman, B.M., Chakravarty, G., Vargo-Gogola, T., Gonzales-Rimbau, M., Hadsell, D.L., Lee, A.V., Settleman, J., and Rosen, J.M. (2007). Crosstalk between the p190-B RhoGAP and IGF signaling pathways is required for embryonic mammary bud development. Dev. Biol. *309*, 137–149.

Kelly, P.A., Bachelot, A., Kedzia, C., Hennighausen, L., Ormandy, C.J., Kopchick, J.J., and Binart, N. (2002). The role of prolactin and growth hormone in mammary gland development. Mol. Cell. Endocrinol. *197*, 127–131.

Kleinberg, D.L., and Ruan, W. (2008). IGF-I, GH, and sex steroid effects in normal mammary gland development. J. Mammary Gland Biol. Neoplasia *13*, 353–360.

Kretzschmar, K., and Watt, F.M. (2012). Lineage tracing. Cell *148*, 33–45.

Lafkas, D., Rodilla, V., Huyghe, M., Mourao, L., Kiaris, H., and Fre, S. (2013). Notch3 marks clonogenic mammary luminal progenitor cells in vivo. J. Cell Biol. *203*, 47–56.

Li, Z., Tognon, C.E., Godinho, F.J., Yasaitis, L., Hock, H., Herschkowitz, J.I., Lannon, C.L., Cho, E., Kim, S.J., Bronson, R.T., et al. (2007). ETV6-NTRK3 fusion oncogene initiates breast cancer from committed mammary progenitors via activation of AP1 complex. Cancer Cell *12*, 542–558.

Meuwissen, R., Linn, S.C., van der Valk, M., Mooi, W.J., and Berns, A. (2001). Mouse model for lung tumorigenesis through Cre/lox controlled sporadic activation of the K-Ras oncogene. Oncogene *20*, 6551–6558.

Puzio-Kuter, A.M., Castillo-Martin, M., Kinkade, C.W., Wang, X., Shen, T.H., Matos, T., Shen, M.M., Cordon-Cardo, C., and Abate-Shen, C. (2009). Inactivation of p53 and Pten promotes invasive bladder cancer. Genes Dev. *23*, 675–680.

Reinert, R.B., Kantz, J., Misfeldt, A.A., Poffenberger, G., Gannon, M., Brissova, M., and Powers, A.C. (2012). Tamoxifen-induced Cre-loxP recombination is prolonged in pancreatic islets of adult mice. PLoS ONE *7*, e33529.

Rios, A.C., Fu, N.Y., Lindeman, G.J., and Visvader, J.E. (2014). In situ identification of bipotent stem cells in the mammary gland. Nature *506*, 322–327.

Russell, T.D., Fischer, A., Beeman, N.E., Freed, E.F., Neville, M.C., and Schaack, J. (2003). Transduction of the mammary epithelium with adenovirus vectors in vivo. J. Virol. *77*, 5801–5809.

Šale, S., Lafkas, D., and Artavanis-Tsakonas, S. (2013). Notch2 genetic fate mapping reveals two previously unrecognized mammary epithelial lineages. Nat. Cell Biol. *15*, 451–460.

Shackleton, M., Vaillant, F., Simpson, K.J., Stingl, J., Smyth, G.K., Asselin-Labat, M.L., Wu, L., Lindeman, G.J., and Visvader, J.E. (2006). Generation of a functional mammary gland from a single stem cell. Nature *439*, 84–88.

Sugihara, T.M., Kudryavtseva, E.I., Kumar, V., Horridge, J.J., and Andersen, B. (2001). The POU domain factor Skin-1a represses the keratin 14 promoter independent of DNA binding. A possible role for interactions between Skn-1a and CREB-binding protein/p300. J. Biol. Chem. *276*, 33036–33044.

Sutherland, K.D., Proost, N., Brouns, I., Adriaensen, D., Song, J.Y., and Berns, A. (2011). Cell of origin of small cell lung

cancer: inactivation of Trp53 and Rb1 in distinct cell types of adult mouse lung. Cancer Cell *19*, 754–764.

Tognon, C., Knezevich, S.R., Huntsman, D., Roskelley, C.D., Melnyk, N., Mathers, J.A., Becker, L., Carneiro, F., MacPherson, N., Horsman, D., et al. (2002). Expression of the ETV6-NTRK3 gene fusion as a primary event in human secretory breast carcinoma. Cancer Cell *2*, 367–376.

van Amerongen, R., Bowman, A.N., and Nusse, R. (2012). Developmental stage and time dictate the fate of Wnt/β-catenin-responsive stem cells in the mammary gland. Cell Stem Cell *11*, 387–400.

Van Keymeulen, A., Rocha, A.S., Ousset, M., Beck, B., Bouvencourt, G., Rock, J., Sharma, N., Dekoninck, S., and Blanpain, C. (2011). Distinct stem cells contribute to mammary gland development and maintenance. Nature *479*, 189–193.

Zhu, Y., Huang, Y.F., Kek, C., and Bulavin, D.V. (2013). Apoptosis differently affects lineage tracing of Lgr5 and Bmi1 intestinal stem cell populations. Cell Stem Cell *12*, 298–303.

Stem Cell Reports, Volume *2*

Supplemental Information

Lineage Tracing of Mammary Epithelial Cells Using Cell-Type-Specific Cre-Expressing Adenoviruses

Luwei Tao, Maaike P.A. van Bragt, Elizabeth Laudadio, and Zhe Li

Supplemental Figures

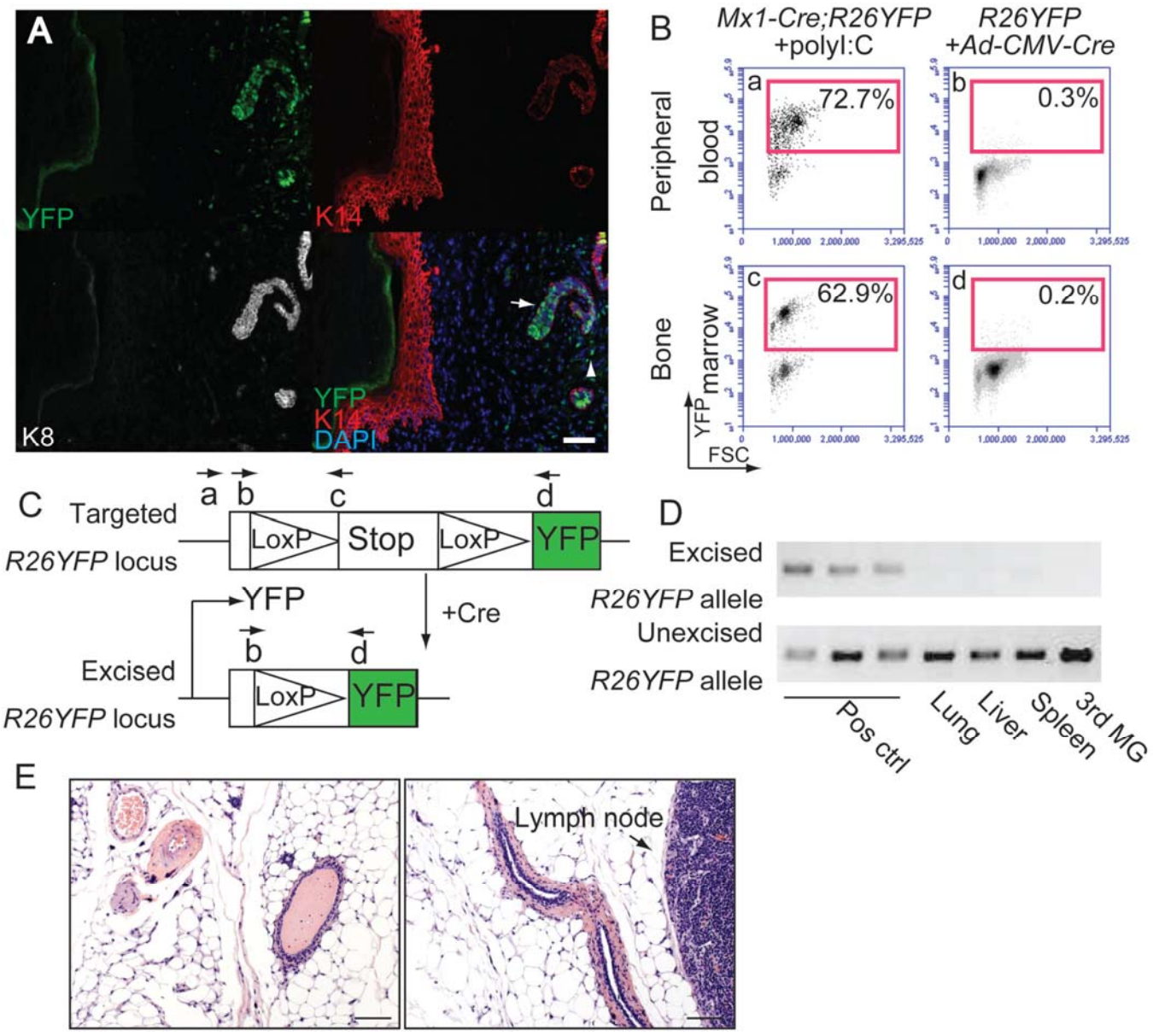

Figure S1-related to Figure 1. Characterization of *Ad-Cre* intraductal injection to mammary glands

(A) IF staining of skin surrounding the nipple area from a *R26YFP* female injected with *Ad-CMV-Cre*. YFP^+ cells can be detected in mammary ducts (arrow) and a few stromal cells (arrowhead) around the ducts. But skin cells (red $K14^+$ cells) were YFP^-. Scale bar = 50μm. **(B)** FACS (fluorescence-activated cell sorting) analysis of peripheral blood and bone marrow from *R26YFP* mice injected with *Ad-CMV-Cre*. Compared to *Mx1-Cre;R26YFP* control mice induced with poly(I:C), no obvious YFP^+ populations were detected in the peripheral blood and bone marrow of *R26YFP* mice injected with *Ad-CMV-Cre* (to their mammary glands). **(C)** Schematic diagram of primers designed to detect the unexcised *R26YFP* conditional knockin allele (primers a+c) and the excised *R26YFP* allele [i.e., YFP activated due to Cre-mediated excision of the floxed *Stopper* cassette (Stop), primers b+d]. **(D)** PCR for detection of Cre-mediated recombination at the *R26YFP* knockin allele using genomic DNA. Positive control DNA samples (Pos ctrl) were isolated from the 4^{th} mammary glands injected with *Ad-CMV-Cre*. Lung, liver, spleen and the 3^{rd} mammary gland (not injected with *Ad-CMV-Cre*) tissues were isolated from one of the *Ad-CMV-Cre* injected animals. **(E)** Hematoxylin & eosin (H&E) staining of mammary gland sections. No obvious inflammation was detected in mammary gland injected with adenovirus except the enlarged lymph node (arrow, 3 days after injection), which eventually reverted to normal size. Scale bar = 50μm.

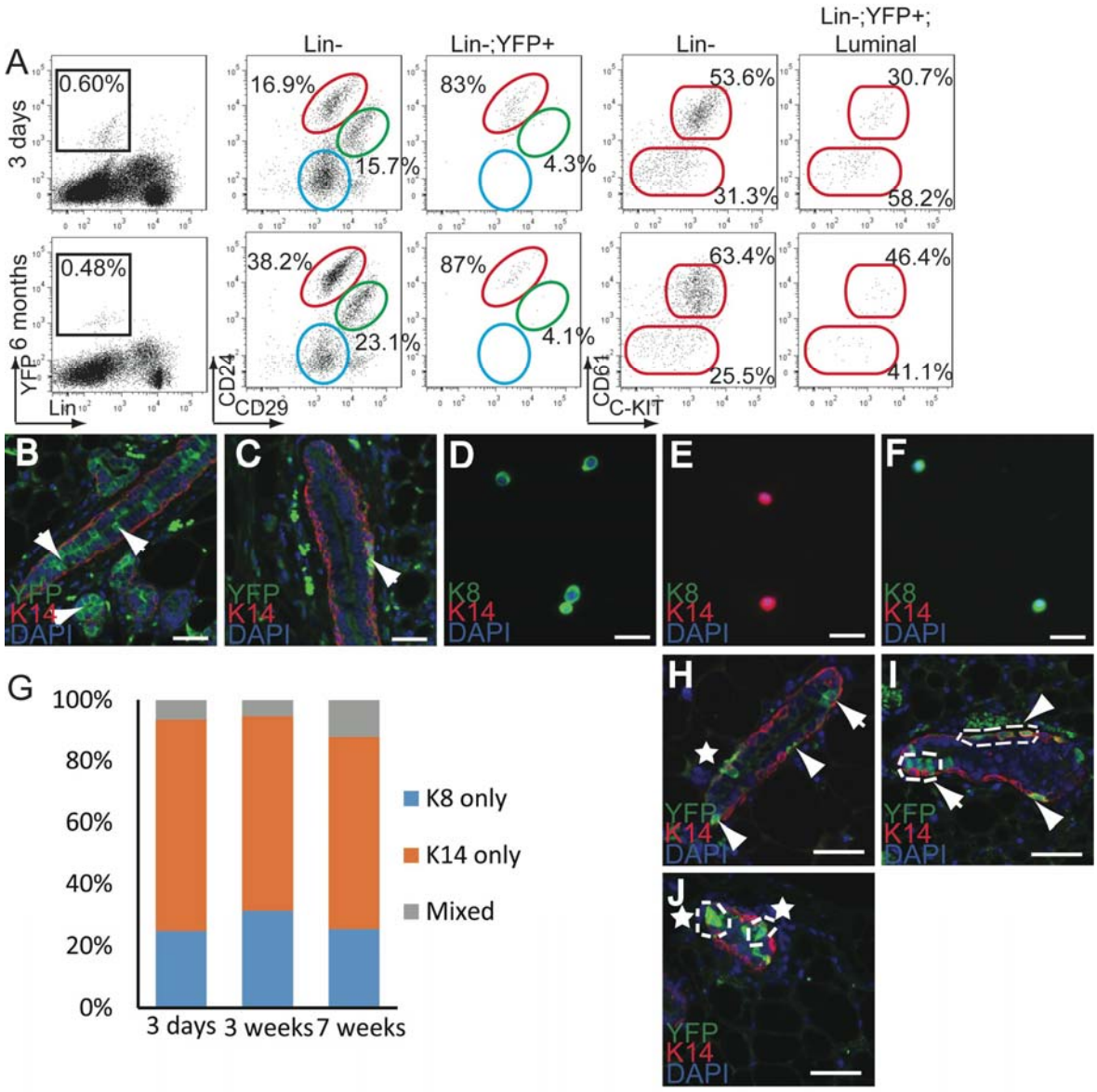

Figure S2-related to Figure 2. Lineage specificity of *Ad-K8-nlsCre* or *Ad-K14-nlsCre* induced genetic marking

(A) FACS analysis of *R26YFP*-only females injected with *Ad-K8-nlsCre* chased for 3 days or 6 months. YFP-marked MECs were restricted to the luminal gate (red circle, middle plot) and included both $CD61^+$ and $CD61^-$ luminal cells (right plot). **(B-C)** Mid-gestation mammary glands chased upon *Ad-K8-nlsCre* or *Ad-K14-nlsCre* injection at the nulliparous stage: **(B)** YFP^+ cells marked by *Ad-K8-nlsCre* at the nulliparous stage contributed to both ductal luminal (white arrows) and alveolar luminal (white arrowhead) cells. **(C)** YFP^+ ductal myoepithelial cells induced by *Ad-K14-nlsCre*. Scale bars = 50μm. **(D-F)** FACS sorted Lin^-YFP^+ cells from mammary glands injected with *Ad-K8-nlsCre* or *Ad-K14-nlsCre*: **(D)** Lin^-YFP^+ cells induced by *Ad-K8-nlsCre* are $K8^+K14^-$. **(E)** $K8^-K14^+$ cells (in the basal gate) induced by *Ad-K14-nlsCre*. **(F)** $K8^+K14^-$ cells (in the luminal gate) induced by *Ad-K14-nlsCre*. Scale bars = 50μm. **(G)** YFP-marked clones induced by *Ad-K14-nlsCre* subdivided based on K8 and K14 expression patterns were quantified as $K8^+K14^-$ (K8 only) clones, $K14^+K8^-$ (K14 only) clones, and Mixed clones with both $K8^+K14^-$ cells and $K14^+K8^-$ cells. Total clones at 3 days (125 clones), 3 weeks (192 clones) and 7 weeks (369 clones) after the initial *Ad-K14-nlsCre* injection were quantified. Quantification of multi-cell clones (at least 3 cells per clone, 31/192 and 134/369 such clones from 3-week and 7-week chase, respectively) is shown in Figure 2H (note at day 3, ~95% clones were 1- or 2-cell clones, therefore its multi-cell clone data was not plotted in Figure 2H**)**. **(H-J)** Representative pictures of clones induced by *Ad-K14-nlsCre*, including K14-only clones (white arrowheads), K8-only clones (white arrows) and Mixed clones (white stars) 3 weeks **(H)** and 7 weeks **(I-J)** after adenovirus injection. Multi-cell clones are indicated by dash lines. Scale bars = 50μm.

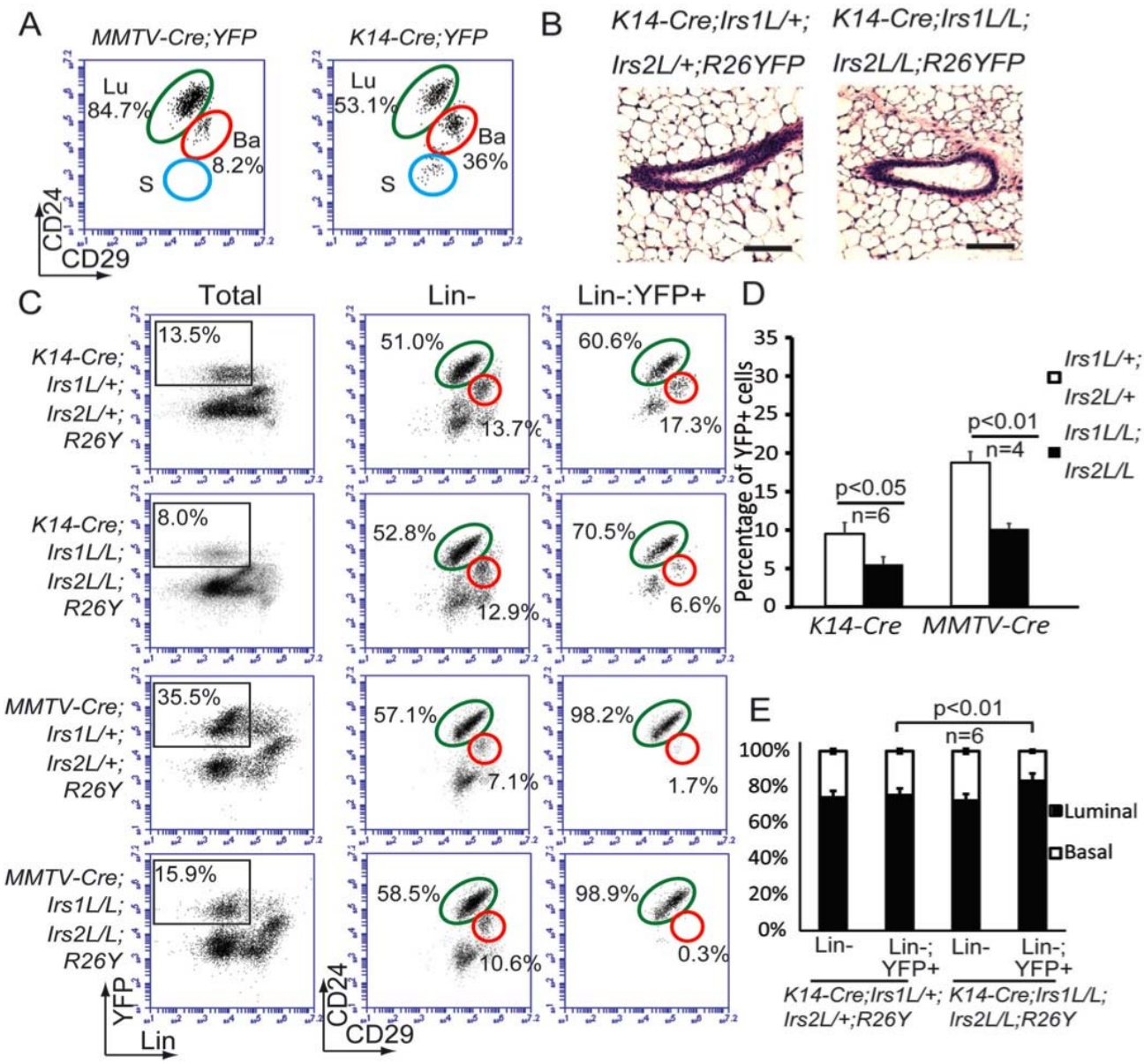

Figure S3-related to Figure 3. IRS1 and IRS2 are essential for maintaining the basal linage in adult mammary glands

(A) FACS analysis (gated for Lin^-YFP^+ cells) of lineage-marking in *R26YFP* females by conventional *K14-Cre* and *MMTV-Cre* transgenic mouse lines. *MMTV-Cre* mainly labels luminal cells (Lu, green circle) and a small number of basal cells (Ba, red circle), whereas *K14-Cre* labels both luminal and basal cells, as well as a small number of stromal cells (S, blue circle). **(B)** H&E staining of *K14-Cre;Irs1$^{L/+}$;Irs2$^{L/+}$;R26YFP* and *K14-Cre;Irs1$^{L/L}$;Irs2$^{L/L}$;R26YFP* female mammary glands showing normal morphology. Scale bars = 50μm. **(C)** *K14-Cre;Irs1$^{L/L}$;Irs2$^{L/L}$; R26YFP* and *MMTV-Cre;Irs1$^{L/L}$;Irs2$^{L/L}$;R26YFP* females had significant reduction in their YFP-marked (thus *Irs1/2*-null) MEC populations (left FACS plots); in addition, they also exhibited more profound decrease in their YFP-marked basal/myoepithelial population compared to that of the YFP^+ luminal cells (right FACS plots), compared to double heterozygous control females. **(D)** Quantification of decrease of Lin^-YFP^+ populations in *K14-Cre;Irs1$^{L/L}$;Irs2$^{L/L}$; R26YFP* and *MMTV-Cre;Irs1$^{L/L}$;Irs2$^{L/L}$;R26YFP* females compared to *K14-Cre;Irs1$^{L/+}$;Irs2$^{L/+}$; R26YFP* and *MMTV-Cre;Irs1$^{L/+}$;Irs2$^{L/+}$; R26YFP* double heterozygous control females. **(E)** Quantification of decrease of Lin^-YFP^+ basal populations in *K14-Cre;Irs1$^{L/L}$;Irs2$^{L/L}$; R26YFP* females compared to *K14-Cre;Irs1$^{L/+}$;Irs2$^{L/+}$; R26YFP* double heterozygous control females. *P* value is indicated.

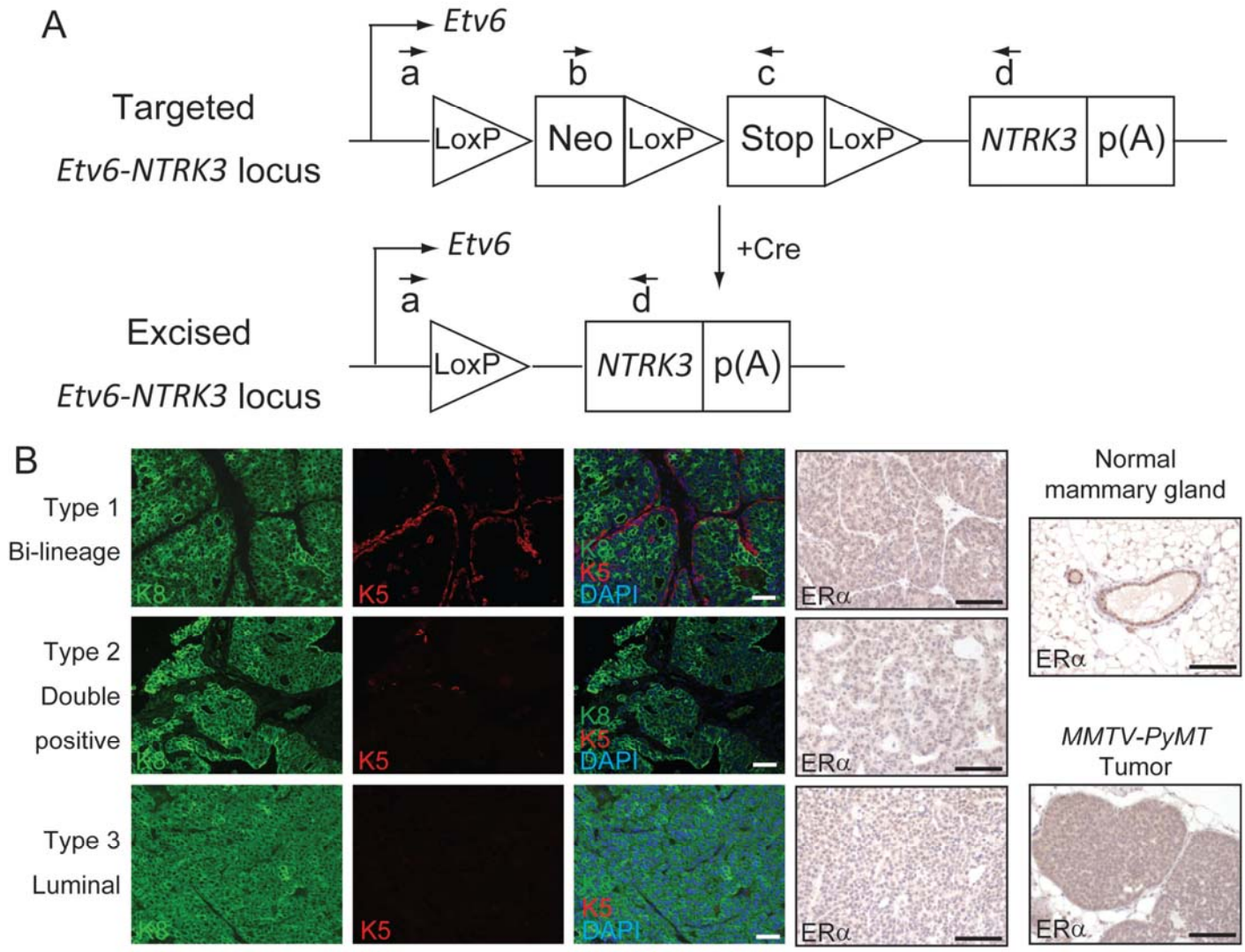

Figure S4-related to Figure 4. Characterization of EN mammary tumors induced by *Ad-K8-nlsCre*

(A) Schematic diagram of primers designed to detect the targeted *EN* conditional knockin allele (unexcised, primers b+c) and the excised *EN* allele (i.e., activated, primers a+d). **(B)** K5/K8 IF staining and ERα IHC staining of three types of mammary tumors developed in *EN/+* female mice injected with *Ad-K8-nlsCre*. ERα IHC staining of a normal mammary gland section (positive control) and a tumor section from an *MMTV-PyMT* female (negative control) were also shown. Note ERα staining intensities in EN mammary tumors were much lower than that of ER^+ cells in normal mammary gland (dark brown cells) and were largely comparable to that of *MMTV-PyMT* luminal tumor; some EN tumors (e.g., Type 1) contain tumor cells with slightly higher ERα staining intensity than those in *MMTV-PyMT* tumor. Scale bars = 50μm.

Supplemental Experimental Procedures

PCR and primers

Gene fragments, including nlsCre coding sequence, mouse *Keratin 8* promoter and human *Keratin 14* promoter, were amplified using Phusion High-Fidelity DNA polymerase (M0530L, New England Biolabs) and the following primers:

nlsCre forward: 5'-CCGACTCTAGCGGCCGCACCATGCCCAAGAAGAAGAGG-3'

nlsCre reverse: 5'-CGAAGCCGGCCGTCGACCTAATCGCCATCTTCC-3'

K8 forward: 5'-GGATGTGTTTAAACGGTGGATCACTTGCCCCCTCCGTTTG-3'

K8 reverse: 5'-AGCTGCTTCGCGGCCGCGGGACAGCGCCCAGCGAAGGCCC-3'

K14 forward: 5'-CTGTTCCGTTTAAACGGGCTCCGGAGCTTCTATTC-3'

K14 reverse: 5'-TGAGTGAAGGCGGCCGCCTCGGGTAAATTGGAAAGGG-3'

The *Stopper* excised and unexcised *R26YFP* (Figure S1C) and *Etv6-NTRK3 (EN)* (Figure S4A) conditional knockin alleles were assessed by PCR by using Taq 5X master mix (M0285s, New England Biolabs) and the following gene specific primers:

R26YFP allele (Figure S1C):

R26YFP-a: 5'-AAAGTCGCTCTGAGTTGTTAT-3'

R26YFP-b: 5'-GACGGTATCGTAGAGTCGAG-3'

R26YFP-c: 5'-GCGAAGAGTTTGTCCTCAACC-3'

R26YFP-d: 5'-CCGGACACGCTGAACTTGTG-3'

Etv6-NTRK3 (EN) allele (Figure S4A):

EN-a: 5'-AGCGTCTCAGTGTATATGGATATG-3'

EN-b: 5'-ACCGCATTAAAGCTTGGCTGGAC-3'

EN-c: 5'-TGGCAAGTGGTATTCCGTAAGAAC-3'

EN-d: 5'-CCGCACACTCCATAGAACTTGAC-3'

Mammary epithelial cell preparation, flow cytometry and sorting

Adenoviruses [diluted in injection medium (DMEM supplemented with 0.1% Bromophenol blue and 0.01M $CaCl_2$)] were introduced into mammary ducts via intraductal injection. The #4 MGs were dissected from injected animals at different time points after intraductal injection. After mechanical dissociation with a sharp scissors, the tissue were placed in digestion media for 1.5h at 37°C (Shackleton et al., 2006). The resultant organoid suspension was sequentially dissociated in 0.25% Trypsin-EDTA for 2min, 1mg/ml DNase for 2min and suspended in red blood cell lysis buffer for 2 min before passing through 40μm cell strainer. The resultant single MEC suspension was subjected to antibody labeling in 96-well plates. Fluorophore-conjugated antibodies were purchased from eBiosciences unless otherwise specified, including CD31-Biotin (clone 390), TER119-Biotin (clone Ter-119), CD45-Biotin (clone 30-F11), CD24-PE (clone M1/69), CD24-eFluor450 (clone M1/69), CD24-eFluor605NC (clone M1/69), CD29-APC (clone eBioHMb1-1), CD49f-APC (clone EbioGoH3), CD61-PE (clone 2C9.G3), C-KIT-PE-Cy7 (clone 2B8). Antibody incubation was performed at 4^oC for 10min. Flow cytometric analysis was performed on Accuri 6 and DXP11 flow cytometers. Cell Sorting was performed on BD Aria. Unstained cells were used to set up the negative gate and single color-stained cells were used to adjust compensation and/or set up the positive gate.

Immunostaining and clonal analysis

Tissue sections were deparaffinized and rehydrated using standard methods. Antigens were retrieved in 10mM sodium citrate buffer, pH6.0. For immunostaining, slides were blocked with 3% H_2O_2/Methanol to inhibit endogenous peroxidase. After 0.5% BSA/PBS blocking for 1 hour, slides was incubated for 1 hour at room temperature using one of the following antibody:

anti-Keratin 5 (Covance, PRB-160P, 1:1000)

anti-Keratin 14 (Covance, PRB-155P or SIG-3476, 1:1000)

anti-Keratin 8 (Covance, MMS-162P, 1:1000)

anti-GFP/YFP (Abcam, ab290, 1:1000)

The secondary antibodies used in IF staining were goat anti-mouse IgG conjugated with AF488 (A11029) or with AF647 (A31571), goat anti-rabbit IgG conjugated with AF488 (A11008), and goat anti-chicken IgG conjugated with AF594 (A11042) (all from Molecular Probes). For IHC staining of ERα, slides were incubated with ERα antibody (Santa Cruz Biotechnology, SC-542, 1:200) followed by detection using ImmPRESS Reagent kit (Vector, MP-7401).

For clonal analysis, after chased for a defined time period, *Ad-Cre*-injected MGs were fixed, embedded in paraffin and the whole MG was sectioned as sagittal sections. After staining for YFP, Keratin 8 (K8) and Keratin 14 (K14), single or clusters of YFP^+ cells that contact each other were defined as YFP-marked clones and their clone types were determined according to their Keratin-staining patterns (i.e., K8-only, or K14-only, or Mixed clones). Clones were further separated by the number of cells per clone and were scored. 3-4 MGs (biological replicates) for each time point were analyzed and their clone data were pooled together based on their clone types, and the frequency of each clone type was calculated as the percentage of the total number of clones, as described previously (Van Keymeulen et al., 2011).

Supplemental References

Shackleton, M., Vaillant, F., Simpson, K.J., Stingl, J., Smyth, G.K., Asselin-Labat, M.L., Wu, L., Lindeman, G.J., and Visvader, J.E. (2006). Generation of a functional mammary gland from a single stem cell. Nature *439*, 84-88.

Van Keymeulen, A., Rocha, A.S., Ousset, M., Beck, B., Bouvencourt, G., Rock, J., Sharma, N., Dekoninck, S., and Blanpain, C. (2011). Distinct stem cells contribute to mammary gland development and maintenance. Nature *479*, 189-193.